Fractal fits to Riemann zeros

Paul B. Slater

Abstract: Wu and Sprung (*Phys. Rev. E*, **48**, 2595 (1993)) reproduced the first 500 nontrivial Riemann zeros, using a one-dimensional local potential model. They concluded — as did van Zyl and Hutchinson (*Phys. Rev. E*, **67**, 066211 (2003)) — that the potential possesses a fractal structure of dimension $d = 3/2$. We model the nonsmooth fluctuating part of the potential by the alternating-sign sine series fractal of Berry and Lewis $A(x, \gamma)$. Setting $d = 3/2$, we estimate the frequency parameter (γ), plus an overall scaling parameter (σ) that we introduce. We search for that pair of parameters (γ, σ) that minimizes the least-squares fit $S_n(\gamma, \sigma)$ of the lowest n eigenvalues — obtained by solving the one-dimensional stationary (nonfractal) Schrödinger equation with the trial potential (smooth plus nonsmooth parts) — to the lowest n Riemann zeros for $n = 25$. For the additional cases, we study, $n = 50$ and 75, we simply set $\sigma = 1$. The fits obtained are compared to those found by using just the smooth part of the Wu–Sprung potential without any fractal supplementation. Some limited improvement — 5.7261 versus 6.392 07 ($n = 25$), 11.2672 versus 11.7002 ($n = 50$), and 16.3119 versus 16.6809 ($n = 75$) — is found in our (nonoptimized, computationally bound) search procedures. The improvements are relatively strong in the vicinities of $\gamma = 3$ and (its square) 9. Further, we extend the Wu–Sprung semiclassical framework to include higher order corrections from the Riemann–von Mangoldt formula (beyond the leading, dominant term) into the smooth potential.

PACS Nos.: 02.10.De, 03.65.Sq, 05.45.Df, 05.45.Mt

Résumé : Utilisant un potentiel local à une dimension, Wu et Sprung (*Phys. Rev. E* **48**, 2595 (1993)) ont reproduit les premiers 500 zéros de Riemann non triviaux. Ils ont conclu — ainsi que van Zyl et Hutchinson (*Phys. Rev. E* **67**, 066211, (2003)) — que le potentiel possède une structure fractale de dimension $d = 3/2$. Nous modélisons la partie de ce potentiel qui n'est pas douce à l'aide de la série sine fractale à signe alterné de Berry et Lewis $A(x, y)$. Fixant $d = 3/2$, nous estimons le paramètre de fréquence (γ), en plus d'un paramètre global d'échelle (σ) que nous introduisons. Nous recherchons la paire de paramètres (γ, σ) qui minimise l'ajustement en moindres carrés $S_n(\gamma, \sigma)$ des n plus basses valeurs propres — obtenues en solutionnant l'équation de Schrodinger stationnaire non fractale à une dimension avec le potentiel d'essai (parties douce et non douce) — aux n plus bas zéros de Riemann pour $n = 25$. Nous étudions aussi les cas $n = 50$ et 75, avec $\sigma = 1$. Les résultats obtenus sont comparés à ceux obtenus en utilisant seulement la partie douce du potentiel de Wu–Sprung sans aucun ajout fractal. Nous observons une certaine amélioration — 5,7261 versus 6,392 07 ($n = 25$), 11,2672 versus 11,7002 ($n = 50$) et 16,3119 versus 16,6809 ($n = 75$) (dans notre recherche qui n'est pas optimisée et a des limites de calcul). Les améliorations sont relativement importantes au voisinage de $\gamma = 3$ et 9 (son carré). De plus, nous avons étendu le cadre de l'approche semi-classique de Wu–Sprung pour inclure des corrections

Received 7 June 2006. Accepted 23 March 2007. Published on the NRC Research Press Web site at http://cjp.nrc.ca/ on 11 May 2007.

P.B. Slater. ISBER, University of California, Santa Barbara, CA 93106, USA (e-mail: slater@kitp.ucsb.edu).

 doi: 10.1139/P07-050

d'ordre plus élevé provenant de la formule de Riemann–van Mangoldt (au delà du premier terme qui est dominant) dans le potentiel doux.

[Traduit par la Rédaction]

1. Introduction

In summarizing the results of their paper, "Riemann zeros and a fractal potential", Wu and Sprung, (ref. 1 p. 2597) stated that

> we have found analytically a one-dimensional local potential which generates the smooth average level density obeyed by the Riemann zeros. We have then shown how any finite number of low lying Riemann zeros can be reproduced by introducing fluctuations on top of the potential. The mystery of how a one-dimensional integrable system can produce a 'chaotic' spectrum is resolved by adopting the concept of a fractal potential which, in the infinite N limit, would lead to the system having a dimension larger than one

(cf. refs. 2–8). ("Indeed …finding an Hermitian operator whose eigenvalues are [the Riemann zeros] may be impossible without introducing chaotic systems" ref. 2 p. 3.)

The Wu–Sprung potential V — which generates the smooth average level density obeyed by the Riemann zeros — satisfied Abel's integral equation, eq. (6) of ref. 1, and was written implicitly as eq. (7) of ref. 1 (cf. ref. 9 and Sect. 4 of ref. 10),

$$x_{\mathrm{WS}}(V) = \frac{1}{\pi}\left(\sqrt{V - V_0}\,\ln\frac{V_0}{2\pi e^2} + \sqrt{V}\,\ln\frac{\sqrt{V} + \sqrt{V - V_0}}{\sqrt{V} - \sqrt{V - V_0}}\right) \tag{1}$$

Here, $V_0 = 3.100\,73\pi \approx 9.741\,23$.

Our objective is to reproduce, as best we can, the fluctuations on top of the potential $V_{\mathrm{WS}}(x)$, implicitly given by (1), so that the application of the Schrödinger equation to the so-amended (smooth plus fractal) potential would yield the Riemann zeros themselves. For our exploratory purposes, we adopt (being a particular case of a deterministic Weierstrass–Mandelbrot (WM) fractal function) the alternating-sign sine series of Berry and Lewis, eq. (5) of ref. 11,

$$A(x, \gamma) = \Sigma_{m=-\infty}^{\infty} \frac{(-1)^m \sin \gamma^m x}{\gamma^{(2-d)m}}, \qquad 1 < d < 2, 1 < \gamma \tag{2}$$

Here, d is the fractal dimension, which — following the box-counting argument of Wu and Sprung [1] (cf. ref. 12) — we take to be 3/2. We have, in this $d = 3/2$ Berry–Lewis context, a specific case,

$$A(\gamma x, \gamma) = -\gamma^{1/2} A(x, \gamma) \tag{3}$$

of the "affine scaling law", eq. (3) of ref. 11. We also scale — in the first ($n = 25$) of our three sets of analyses ($n = 25, 50, 75$) — $A(x, \gamma)$ by a parameter σ, where n is the number of the lowest Riemann zeros we aspire to fit (Sect. 2.1). For the cases $n = 50$ (Sect. 2.2) and 75 (Sect. 2.3), we will simply set $\sigma = 1$. In Sect. 3, we demonstrate how to incorporate more terms of the Riemann–von Mangoldt formula [13] for the cumulated number of Riemann zeros than Wu–Sprung themselves did, using a semiclassical argument, in deriving $x_{\mathrm{WS}}(V)$. (It remains, however, to implement numerically these last findings.)

2. Analyses

2.1. $n = 25$

We proceed, to begin, trying to fit the first 25 Riemann zeros by finding distinguished values of the two parameters (γ and σ). We randomly generate trial values $1 \leq \gamma \leq 10$ and $0 \leq \sigma < 10$.

Fig. 1. Deviations from the first 25 Riemann zeros of the first 25 eigenvalues obtained by solving the Schrödinger equation using the (smooth and (or) nonfractal) Wu–Sprung potential (1). The sum-of-squares of these deviations is 6.392 07, while the sum-of-squares of these Riemann zeros is much larger, 92 569.63.

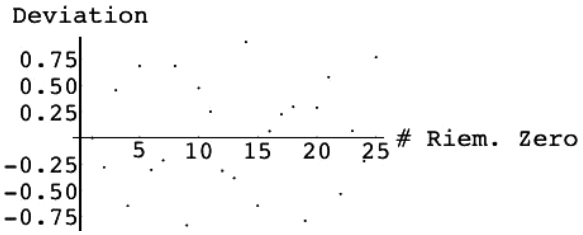

Fig. 2. Scatterplot showing the sum-of-squares goodness-of-fit statistic $S_{25}(\gamma, \sigma)$ as a function of the frequency parameter (γ) and the scaling parameter (σ). Those 1833 points of the 4007 sampled for which $S_{25}(\gamma, \sigma) < 15$ are included.

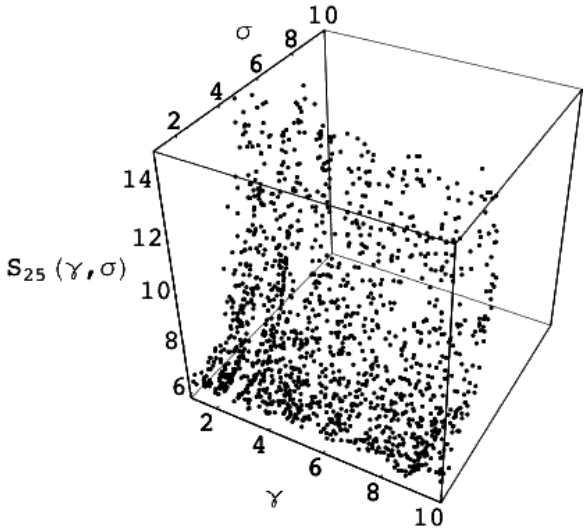

(Numerically speaking, we truncate the summation in (2) by summing from $m = -30$ to $m = 30$ (cf. App. of ref. 11). We have not yet gauged the sensitivity of the various results in this paper to this choice of cutoff — nor to the setting $d = 3/2$ nor further to the specific measure of fit (sum-of-square deviations) employed — though it would certainly be of interest to do so for any or all of them.)

If we use the smooth potential given by (1) itself — without any fractal supplementation — the sum-of-squares deviation of the first 25 eigenvalues yielded by application of the one-dimensional stationary Schrödinger equation from the first 25 Riemann zeros is 6.239 07 (Fig. 1). (This is only 0.0069% of the total (nonfitted) sum of squares of the zeros themselves, that is, 92 569.63, so one might aver that the semiclassically based smooth Wu–Sprung potential is notably successful in well-approximating the Riemann zeros. It is, of course, our objective here to reduce this small percentage even further. Let us also note that a referee suggested that the scatter in Figs. 1, 7, and 9 might be reduced if the modulus of the scatter were to be plotted.)

We randomly generated 4007 pairs of (γ, σ) from the indicated ranges, and solved for each such pair, the Schrödinger equation with the smooth potential plus the fractal $\sigma A(x, \gamma)$ with the corresponding choice of γ and σ. Further, we calculated the corresponding sum-of-squares ($S_{25}(\gamma, \sigma)$) deviations from the first 25 Riemann zeros. We obtained a range of values $S_{25}(\gamma, \sigma) \in [5.7261, 166.075]$. In Fig. 2, we

Fig. 3. Truncation of the previous scatterplot to those 210 (fit-improving) pairs yielding $S_{25}(\gamma, \sigma) < 6.392\,07$. For all such pairs $\sigma < 2.864\,75$.

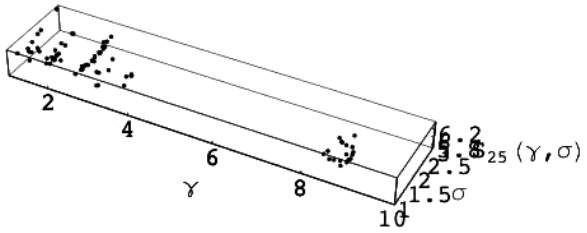

Fig. 4. Histogram for the frequency parameter γ corresponding to those 210 pairs (γ, σ) for which $S_{25}(\gamma, \sigma) < 6.392\,07$, the value obtained from solving the Schrödinger equation using the smooth unsupplemented Wu–Sprung potential. The classification bins for $\gamma \in [1, 9.5]$ are of length 1/2.

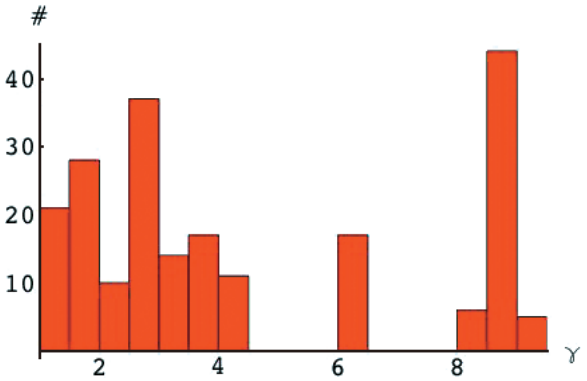

Fig. 5. Histogram for the scaling parameter σ corresponding to those 210 pairs (γ, σ) for which $S_{25}(\gamma, \sigma) < 6.392\,07$.

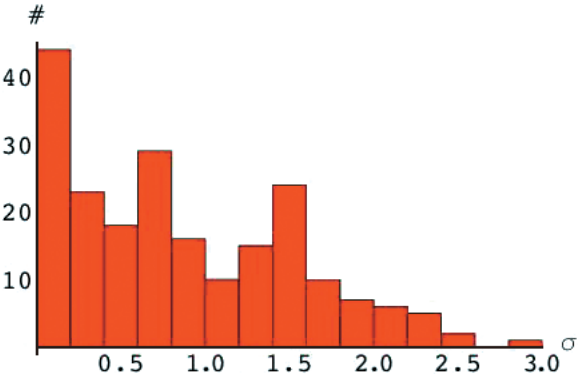

display the results for the 1833 pairs of the 4007 that yielded $S_{25}(\gamma, \sigma) < 15$.

Additionally, in Fig. 3, we show the results for those 210 pairs yielding $S_{25}(\gamma, \sigma) < 6.392\,07$ — that is, those pairs that yield results superior (numerically inferior, that is) to those obtained with the original smooth unsupplemented potential (1). Figure 4 is a histogram of the values of γ — having been uniformly sampled from [1,10] — occurring in these 210 pairs. (There were no γ's recorded for a number of bins, including [9.5,10].) The two topmost peaks (corresponding to the classification bins $\gamma \in [2.5, 3]$ and [8.5,9]) may possibly reflect (cf. (3)) an assertion of Berry and Lewis, made (using t for what we denote by x) in regard to what they termed deterministic Weierstrass–Mandelbrot fractal functions ($W(t)$). They note that "the whole function W can be reconstructed from its values in the

Fig. 6. Plot of those pairs (γ, σ) for which $S_{25}(\gamma, \sigma) < 6.392\,07$. The correlation coefficient is $-0.264\,263$.

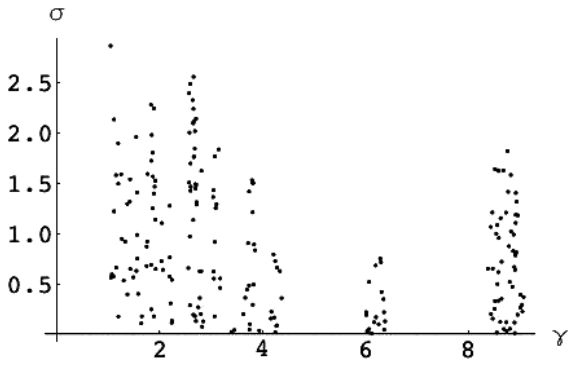

Fig. 7. Deviations from the first 25 Riemann zeros of the first 25 eigenvalues obtained by solving the Schrödinger equation using the (nonfractal) Wu–Sprung potential (1) supplemented by the scaled Berry–Lewis fractal function $1.957\,98A(x, 1.545\,23)$. The sum-of-squares of these deviations is 5.7261, reduced from 6.392 07 for the nonsupplemented smooth potential (Fig. 1).

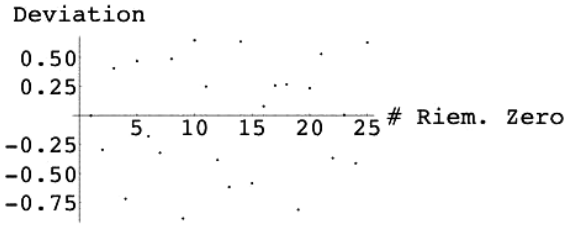

Fig. 8. Eigenfunctions drawn at the eigenvalues obtained by solving the Schrödinger equation for the potential that yields the minimum $S_{25}(1.545\,23, 1.957\,98) = 5.7261$ of the 4,007 pairs sampled.

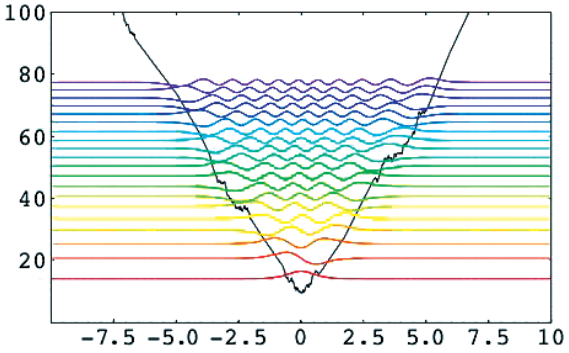

range $t_0 \le t \le \gamma t_0$; for example, W in the ranges $\gamma t_0 \le t \le \gamma^2 t_0$ and $\gamma^{-1} t_0 \le t \le t_0$ are magnified and diminished versions, respectively, of W in the range $t_0 \le t \le \gamma t_0 \ldots$ The repetition and resolution of features at t_0, γt_0, $\gamma^2 t_0$ etc, is again obvious" p. 461 of ref. 11. (Similar γ-histograms — Figs. 12 and 17 — will be obtained for the $n = 50$ and 75 analyses below.)

In Fig. 5, we have an analogous histogram based on the scaling parameter σ. (For no value of $\sigma > 2.864\,75$, though we sample uniformly from [0,10], do we obtain an improvement by using $\sigma A(x, \gamma)$.)

In Fig. 6, we have — for these same 210 pairs — a plot of γ versus σ. (The associated correlation coefficient is negative, that is, $-0.275\,492$.)

Fig. 9. Deviations from the first 50 Riemann zeros of the first 50 eigenvalues obtained by solving the Schrödinger equation using the (nonfractal) Wu–Sprung potential (1). The sum-of-squares of these deviations is 11.7002.

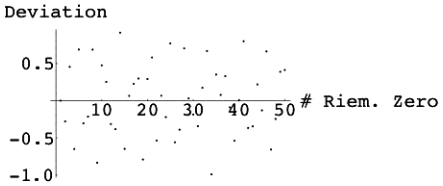

Fig. 10. A "rankit" plot to assess the possible normality of the distribution of deviations of the 50 eigenvalues from the Schrödinger equation solution using the smooth Wu–Sprung potential from the Riemann zeros themselves. For normally-distributed observations, one expects a straight line.

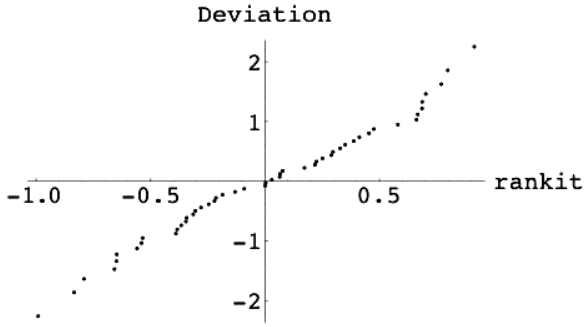

The minimum over all the 4007 pairs was $S_{25}(1.545\,23, 1.957\,98) = 5.7261$. (The next smaller value was $S_{25}(1.152\,74, 1.579\,31) = 5.817\,54$. All other sum-of-squares deviations exceeded 6.0.) In Fig. 7 (cf. Fig. 1), we show the deviations of the predicted eigenvalues at this point (1.152 74,1.579 31) from the corresponding Riemann zeros. In Fig. 8, we display, for this same minimizing point, the corresponding 25 eigenfunctions drawn at the 25 eigenvalues for the associated (smooth plus fractal) potential.

2.2. $n = 50$

Now, we present in Fig. 9 the extension of Fig. 1 from the first 25 to the first 50 Riemann zeros. (It is considerably more demanding to solve the Schrödinger equation for this increased n.) The associated sum-of-squares is 11.7002, which is but 0.002 61% of the total sum-of-squares, 448 704.56, of the first 50 Riemann zeros themselves.

In Fig. 10, we show the results of a "rankit" test (described in the Wikipedia on-line encyclopaedia) for the normality of the distribution of deviations in Fig. 9. If the observations do come from a normal and (or) Gaussian distribution, we expect the plot (necessarily nondecreasing in any case, Gaussian or otherwise) to be a straight line. So, there appears to be some deviations from strict normality, particularly in the tails of the distribution (suggesting that perhaps sums-of-squares might not be the most robust measure of deviation to be employed for evaluation of fits — though it is certainly the most conventional and familiar measure).

We repeated for the case $n = 50$, the form of analysis conducted for $n = 25$ (Sect. 2.1), but now omitting (in the interest of interpretational simplicity) the scaling parameter (σ) — effectively setting it to unity. Based on 1013 random choices of γ lying in [1, 10], we obtained Fig. 11. The minimum achieved was $S_{50}(3.100\,07, 1) = 11.2672$, while without any fractal supplementation at all, the (larger) value of 11.7002 was obtained. (As a matter of curiosity, we found that $S_{50}(1, g_{\mathrm{Au}}) = 11.7641 \geq 11.7002$, where $g_{\mathrm{Au}} = (\sqrt{5}+1)/2 \approx 1.618\,03$ is the golden mean [14]. Interpolation by third-degree polynomials of the points in Fig. 11 suggests that the actual minimum of 11.2556 would be achieved for $\gamma = 3.092$.)

Fig. 11. Scatterplot showing the sum-of-squares goodness-of-fit statistic $S_{50}(\gamma, 1)$, based on 1013 randomly chosen points $0 \leq \gamma \leq 10$. Points below the γ-axis correspond to improvements in fit.

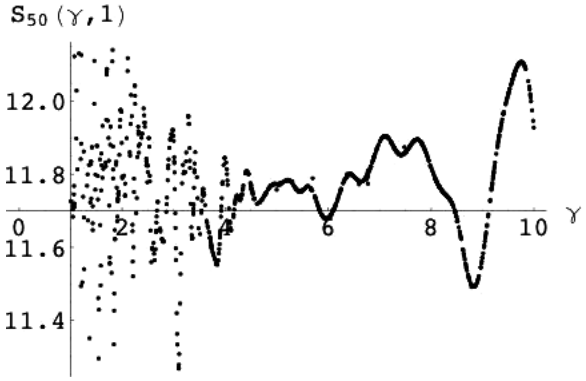

Fig. 12. Histogram corresponding to those 219 values of the frequency parameter γ for which $S_{50}(\gamma, 1) < 11.7002$, the value obtained from solving the Schrödinger equation using the smooth unsupplemented Wu–Sprung potential. The classification bins for $\gamma \in [1, 9.5]$ are of length $1/2$.

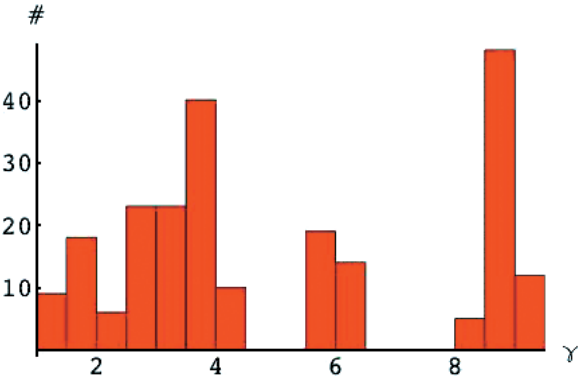

The penultimate minimum, $S_{50}(3.100\,51, 1) = 11.2685$, was nearby. Again (cf. Fig. 4), we appear to discern a manifestation of relative minima in the vicinity of both $\gamma = 3$ and (its square) 9. (Also around $\gamma = 6$, as in Fig. 4 too. The associated relative minimum of 11.678 occurs at $\gamma = 5.961\,58$.) The relative minimum (11.4906) in the vicinity of $\gamma = 9$ was attained at $\gamma = 8.786\,02$, so, at that point, one has $\sqrt{\gamma} = 2.964\,12$. For the smaller values of γ, the plot is very scattered, but for the higher ones, a well-defined curve emerges. (The overall maximum is 12.1412 at $\gamma = 1.8165$, while the maximum in the upper range [8, 10] is 12.108 at $\gamma = 9.7516$.) We applied (third-order) interpolation to the data in Fig. 11 and obtained for the most salient domains of improved fit, $\gamma \in [3.032\,05, 3.1537]$ (containing our overall minimum) and [3.335 83,3.384 88], [5.859 54,6.085 65] and [8.459 62,9.122 72] (containing our three distinct relative minima [Fig. 11]).

In Fig. 12 (cf. Fig. 4), we show the histogram based on those (fit-improving) 219 of the 1013 values of γ for which $S_{50}(\gamma, 1) < 11.7002$. In Fig. 13, we plot the deviations (Δ_{smooth}) from the first 50 Riemann zeros obtained using the smooth potential against those deviations (Δ_{fractal}) using the supplemented potential which minimizes the fit, obtaining basically a linear relationship. In Fig. 14, we have the counterpart of Fig. 8, for the case $n = 50$.

Fig. 13. The predicted eigenvalues minus the first 50 Riemann zeros: the horizontal axis based on the smooth potential and the vertical axis based on the sum-of-squares minimizing fit.

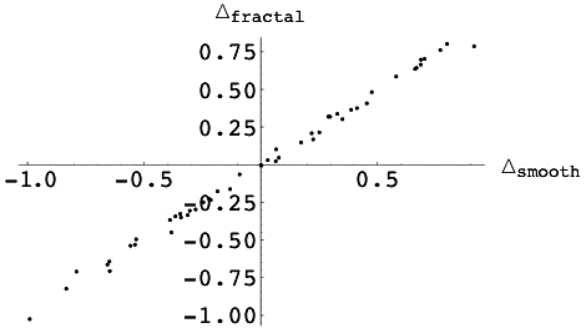

Fig. 14. Eigenfunctions drawn at the eigenvalues obtained by solving the Schrödinger equation for the potential that yields the minimum $S_{50}(3.100\,07, 1) = 11.2672$ of the 1013 points sampled.

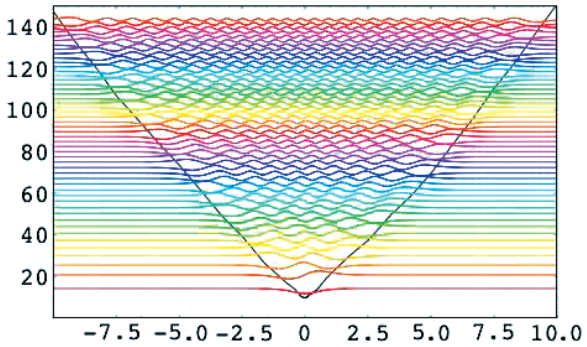

Fig. 15. Deviations from the first 75 Riemann zeros of the first 75 eigenvalues obtained by solving the Schrödinger equation using the (nonfractal) Wu–Sprung potential (1). The sum-of-squares of these deviations is 16.6809.

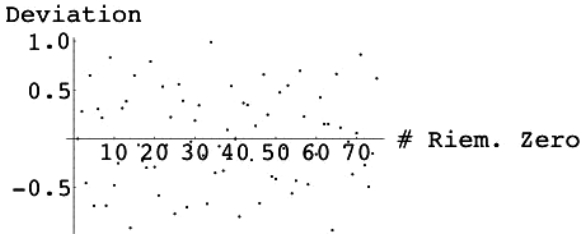

2.3. $n = 75$

Fig. 15 is the further extension of Figs. 1 and 9 to the $n = 75$ case. The associated sum-of-squares is 16.6809, which is but 0.001 4308% of the total sum-of-squares of the first 75 Riemann zeros, $1.165\,8469 \times 10^6$. We generated 853 values of the frequency parameter γ, uniformly sampling from the interval [1,10]. The best fit of 16.3119 was achieved for $\gamma = 3.1106$. (The penultimate minimum of 16.3427 was nearby at $\gamma = 3.116\,32$, while the overall maximum [worse fit] was 19.27 at $\gamma = 2.476\,89$.) In Fig. 16, we plot these 853 values as a function of γ. (In the vicinity of $\gamma = 9$, the relative minimum of 16.5983 is achieved at $\gamma = 8.645\,89 \approx 2.940\,39^2$.) In Fig. 17 we show the corresponding histogram.

Fig. 16. Scatterplot showing the sum-of-squares goodness-of-fit statistic $S_{75}(\gamma, 1)$, based on 853 randomly chosen points $0 \leq \gamma \leq 10$. Points — of which there are 172 — below the γ-axis correspond to improvements in fit.

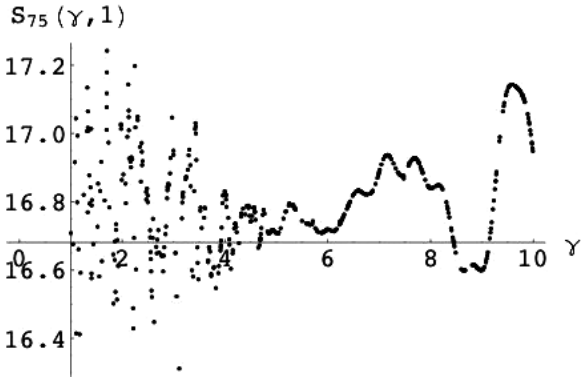

Fig. 17. Histogram corresponding to those 172 values of the frequency parameter γ for which $S_{75}(\gamma, 1) < 16.6809$, the value obtained from solving the Schrödinger equation using the smooth unsupplemented Wu–Sprung potential. The classification bins for $\gamma \in [1, 10]$ are of length 1.

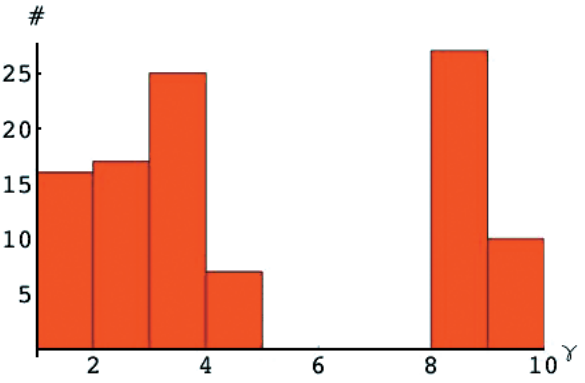

We continue to add randomly generated points to this $n = 75$ analysis, and may possibly undertake an $n = 100$ study too.

3. Higher order corrections to the Wu–Sprung potential

In their semiclassical analysis, Wu and Sprung [1] took into account only the leading term of the Riemann–von Mangoldt formula [13], but nevertheless, as our results indicate, doing so is able to yield, via the Schrödinger equation, eigenvalues that quite closely approximate the Riemann zeros themselves. It might prove beneficial, in trying to account for the (relatively small) residual variation — especially since we have been working in a nonasymptotic regime — to extend the Wu–Sprung approach by incorporating the higher order nonoscillatory terms of the Riemann–von Mangoldt formula too (cf. ref. 15 and eq. 95) of ref. 16).

The (smooth) leading term — of the Riemann–von Mangoldt formula for the number of zeros below E — employed by Wu and Sprung took the form

$$N(E) = \frac{E}{2\pi} \log \frac{E}{2\pi e} + \frac{7}{8} \tag{4}$$

(This formula pertains to the important Connes/Berry–Keating absorption/emission spectrum "sign"

problem, see eqs. (6) and (11) of ref. 17.) The remaining part (having both smooth and nonsmooth components) not utilized by Wu and Sprung is expressible as [13]

$$S(E) + \frac{1}{\pi}\delta(t) \tag{5}$$

where

$$S(E) = \frac{1}{2}\arg\zeta\left(\frac{1}{2} + iE\right) \tag{6}$$

is the argument function and $\zeta(s)$ is the Riemann zeta function. Further,

$$\delta(E) = \frac{E}{4}\log\left(1 + \frac{1}{4E^2}\right) + \frac{1}{4}\arctan\frac{1}{2E} - \frac{E}{2}\int_0^{+\infty}\frac{\rho(u)\,\mathrm{d}u}{(u+1/4)^2 + (E/2)^2} \tag{7}$$

and $\rho(u) = 1/2 - \{u\}$. (Here, $\{u\}$ is the fractional part of u.) The function $S(E)$ is itself strongly oscillatory (changing sign an infinite number of times).

Incorporating the two additional (higher order — $O(E^{-2})$ and $O(E^{-3})$, respectively) nonoscillatory (monotonically decreasing) terms of the Riemann–von Mangoldt formula [13], one could seek to find the potential based on

$$N(E) + \frac{E}{4}\log\left(1 + \frac{1}{4E^2}\right) + \frac{1}{4}\arctan\frac{1}{2E} \tag{8}$$

The corresponding potential can, in fact, be straightforwardly constructed (in implicit form), using the formula for Abel's integral equation [18], following the procedure outlined in [1]. It takes the form

$$\begin{aligned} x_{\mathrm{WS_H}}(x) = {} & \frac{2(1+\pi)\sqrt{V}\tanh^{-1}\left(\frac{\sqrt{V-V_0}}{\sqrt{V}}\right)}{\pi^2} - \frac{2(1+\pi)\sqrt{V-V_0}}{\pi^2} + \frac{2\sqrt{V-V_0}}{\pi^2} \\ & - \frac{V\tanh^{-1}\left(\frac{\sqrt{V-V_0}}{\sqrt{V-\frac{i}{2}}}\right)}{\pi^2\sqrt{V-\frac{i}{2}}} - \frac{V\tanh^{-1}\left(\frac{\sqrt{V-V_0}}{\sqrt{V+\frac{i}{2}}}\right)}{\pi^2\sqrt{V+\frac{i}{2}}} \\ & - \frac{i\left[\frac{\tan^{-1}\left(\frac{\sqrt{2}\sqrt{V-V_0}}{\sqrt{2V_0-i}}\right)}{\sqrt{2V_0-i}} - \frac{\tan^{-1}\left(\frac{\sqrt{2}\sqrt{V-V_0}}{\sqrt{2V_0+i}}\right)}{\sqrt{2V_0+i}}\right]}{\sqrt{2}\pi^2} \\ & - \frac{\left\{\log\left(1+\frac{1}{4V_0^2}\right) + \pi\left[\log\left(4\pi^2\right) - 2\log\left(V_0\right)\right]\right\}\sqrt{V-V_0}}{2\pi^2} \\ & - \frac{i\log\left[\frac{(1-i)V_0+\sqrt{V}}{\left((1+i)\sqrt{V}+i\right)\sqrt{2i-4V_0}} + \frac{2i\sqrt{V-V_0}}{4\sqrt{V}+(2+2i)}\right]}{2\pi^2\sqrt{2i-4V_0}} \end{aligned}$$

Fig. 18. The original (implicitly expressed) Wu–Sprung potential (1) minus the one (9) with higher order Riemann–von Mangoldt corrections.

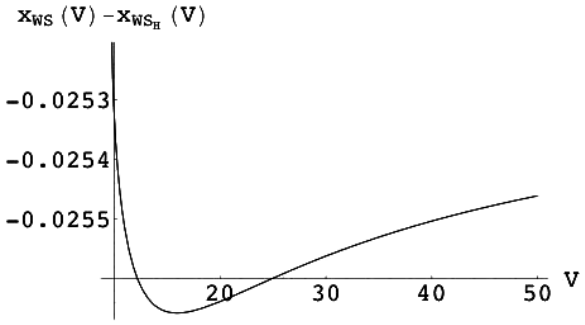

Fig. 19. The original (implicitly expressed) Wu–Sprung potential (1) divided by the one (9) with higher order Riemann–von Mangoldt corrections.

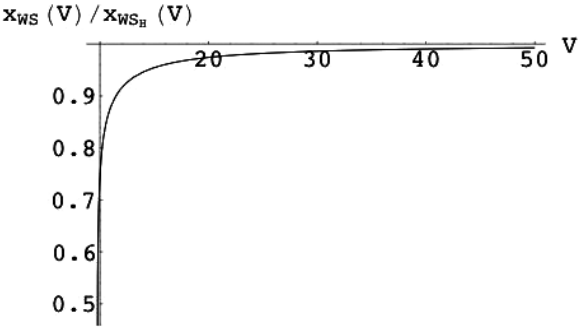

$$+\frac{i\log\left[\frac{(-1+i)V_0-i\sqrt{V}}{\left((1+i)\sqrt{V}-1\right)\sqrt{-4V_0-2i}}-\frac{2i\sqrt{V-V_0}}{4\sqrt{V}-(2-2i)}\right]}{2\pi^2\sqrt{-4V_0-2i}}$$
$$-\frac{i\log\left[\frac{(1-i)\left(\sqrt{i-2V_0}\sqrt{V-V_0}-\sqrt{2}V_0\right)+\sqrt{2}\sqrt{V}}{\left(2i-(2+2i)\sqrt{V}\right)\sqrt{i-2V_0}}\right]}{2\pi^2\sqrt{2i-4V_0}}$$
$$+\frac{i\log\left[\frac{i\left((1+i)V_0+\sqrt{V}\right)}{\left((1+i)\sqrt{V}+1\right)\sqrt{-4V_0-2i}}+\frac{(1-i)\sqrt{V-V_0}}{(2+2i)\sqrt{V}+2}\right]}{2\pi^2\sqrt{-4V_0-2i}} \quad (9)$$

We have not so far been able to numerically invert $x_{\mathrm{WS_H}}(V)$, but in Figs. 18 and 19 we show the difference $x_{\mathrm{WS}}(V) - x_{\mathrm{WS_H}}(V)$ and the ratio $x_{\mathrm{WS}}(V)/x_{\mathrm{WS_H}}(V)$, respectively. (As in the original Wu–Sprung analysis [1], we set $V_0 = 9.741\,23$ in both cases.)

4. Concluding remarks

It might be possibly worthwhile exploring, in our context, the use of fractals other than the specific Berry–Lewis alternating-sign sine series (2) (cf. Chap. 12 of ref. 19 and refs. 20 and 21). (It appears that $A(x, \gamma)$ increases with x, while the Wu–Sprung plots of the fluctuations of the fractal potential from the smooth one, see Fig. 2 of ref. 1, do not seem to exhibit such a growth phenomenon (cf. Figs. 12 and 13 of ref. 19). However, certain quite preliminary efforts of ours to explore along such lines have

encountered some so-far not well-understood numerical difficulties.) Along with the alternating-sign sine series ($A(x, \gamma)$) we have employed, Berry and Lewis too analyzed a certain companion (also deterministic Weierstrass–Mandelbrot) cosine series $C(x, \gamma)$. However, this function can only assume nonnegative values, so — unless translated — it does not provide an immediately suitable model of the Wu–Sprung (both negative and positive) fluctuations.

In the asymptotic limit, the Wu–Sprung potential $V_{\mathrm{WS}}(x)$ behaves as, see, eq. (9) of ref. 9,

$$V_{\mathrm{WS}_{\mathrm{asymp}}}(x) = \frac{\pi^2 x^2}{4}\left[\mathrm{LW}\left(\sqrt{\frac{\pi}{2}}\frac{|x|}{e}\right)\right]^{-2}, \qquad |x| \to \infty \tag{10}$$

where LW(·) represents the Lambert-W function [22]. It would be interesting to explore the question of whether the Schrödinger equation can be exactly solved with (10) as a potential (cf. ref. 23). In regard to this matter, Trott commented that

> I would guess it is enough to look for the asymptotic region. If an analytic solution exists there, one might be able to 'guess' the correct one in terms of Lambert-W. If one can't find an exact solution asymptotically, then probably no exact one in Lambert-W does exist either.

If so, then with the use of perturbation theory [24], one might possibly be able to expedite the computational procedure we have employed above (in which we have solved the Schrödinger equation — a demanding task — ab initio for each new set of random parameters).

Questions pertaining to the nature of the eigenfunctions obtained and of the importance of tunneling contributions in the fractal potential remain to be addressed (cf. Figs. 8 and 14).

Castro and Mahecha — in their proposed supersymmetric model of the Riemann zeros — suggested the use of a "*fractal* [emphasis added] SUSY QM equation instead of factoring the *ordinary* [emphasis added] Schrödinger equation studied by Wu–Sprung" [20] (cf. refs. 21, 25, and 26). They further proposed the use of a fully general Weierstrass–Mandelbrot fractal to model fluctuations in the supersymmetric potential. The alternating-sign sine series fractal (2) we have employed in this study is a specific instance of the WM-fractal [11], involving far fewer parameters — which is largely why we have employed it here in our exploratory numerical analyses. (References to further related work of Castro can be found at the number theory and physics archive website http://secamlocal.ex.ac.uk/people/staff/mrwatkin/zeta/physics.htm.)

The analytical approach of Wu and Sprung [1], which has been the basis of our study here incorporates the familiar ("Berry–Keating" [27]) form of density-of-states $N(E)$ given in (4). However, in Connes's adelic (absorption spectrum) approach [28] the density-of-states takes another (cutoff (Λ)-dependent) form, see eq. (11) of ref. 17,

$$N_{\mathrm{Connes}}(E) = \frac{E}{2\pi}\log\Lambda^2 - \frac{E}{2\pi}\left(\log\frac{E}{2\pi} - 1\right) \tag{11}$$

The question, then, arises of whether or not the Wu–Sprung framework can be meaningfully and (or) differently recast in the Connes adelic setting. (Berry has been quoted to the effect that "we think this is a matter of formalism and everything you can write as an absorption you can write as an emission spectrum if you manipulate things the right way", p. 247 of ref. 29. It has been proposed that the approach of Connes can be implemented using pseudo-Hermitian Hamiltonians for which the eigenvectors are null [30]. Shudo et al. [31] measured absorption spectra and investigated the distribution of eigenfrequencies in "L-shaped" resonators.)

In the context of fractal strings and sprays, the classical Riemann zeta function "can be viewed as the spectral zeta function of the unit interval", p. 2 of ref. 32.

In their study of the Weierstrass–Mandelbrot fractal function, upon which we have strongly relied, Berry and Lewis found, after some delicate analysis, that an attractive inverse-square potential generates

the "Weierstrass spectrum" γ^n, Sect. 5 of ref. 11. They further speculated that there might be no other such potential.

Acknowledgments

I would like to express gratitude to the Kavli Institute for Theoretical Physics (KITP) for computational support, and to Carlos Castro and Michael Trott for their sustained interest and expert advice. M. Trott first implemented the analysis underlying Figs. 1 and 8 and furnished the Mathematica program for solving the Schrödinger equation that was used repeatedly above.

References

1. H. Wu and D.W.L. Sprung. Phys. Rev. E, **48**, 2595 (1993).
2. N.N. Khuri. Math. Phys. Anal. Geom. **5**, 1 (2002).
3. M. Tomiya and S. Sakamoto. e-J. Surf. Sci. Nanotech. **1**, 175 (2003).
4. M. Tomiya, S. Sakamoto, H. Inoue, and N. Yoshinaga. Prog. Theor. Phys. Supp. **157**, 156 (2005).
5. N. Yoshinoga, M. Tomiya, S. Sakamoto, and A. Hirai. Comput. Phys. Commun. **169**, 313 (2005).
6. M. Tomiya and N. Yoshinaga. Prog. Theor. Phys. Supp. **150**, 453 (2003).
7. D.A. Lidar, D. Thirumalai, R. Elber, and R.B. Gerber. Phys. Rev. E, **59**, 2231 (1999).
8. P. Babinec. Chaos Sol. Fract. **22**, 1007 (2004).
9. D. Dominici. Some remarks on the Wu–Sprung potential. Preliminary report, e-print math.CA/0510341.
10. J. Twamley and G.J. Milburn. The quantum mellin transform. e-print quant-ph/0702107.
11. M.V. Berry and Z.V. Lewis. Proc. R. Soc. London A, **370**, 459 (1980).
12. B.P. van Zyl and D.A.W. Hutchinson. Phys. Rev. E, **67**, 066211 (2003).
13. A.A. Karatsuba and M.A. Korolev. Russian Math. Surveys, **60**, 433 (2005).
14. M. Livio. The golden ratio. Broadway, New York. 2002.
15. K. Weibert, J. Main, and G. Wunner. Eur. Phys. J. D, **19**, 379 (2002).
16. J. Main, V.A. Mandelshtam, G. Wunner, and H.S. Taylor. Nonlinearity, **11**, 1015 (1998).
17. G. Sierra. J. Statist. Mech. **2005**, P12006 (2005).
18. R. Gorenflo and S. Vessalla. Abel integral equations: Analysis and applications. Springer-Verlag, Berlin. 1990.
19. C. Tricot. Curves and fractal dimensions. Springer-Verlag, New York. 1995.
20. C. Castro and J. Mahecha. Int. J. Geom. Methods Mod. Phys. **1**, 751 (2004).
21. P.B. Slater. A numerical examination of the Castro–Mahecha supersymmetric model of the Riemann zeros. e-print math.NT/0511188.
22. R.M. Corless, G.H. Gonnet, D.E.G. Hare, D.J. Jeffrey, and D.E. Knuth. Adv. Comput. Math. **5**, 329 (1996).
23. B.W. Williams. Phys. Lett. **334A**, 117 (2005).
24. T. Kato. Perturbation theory for linear operators. Springer-Verlag, Berlin. 1966.
25. N. Laskin. Phys. Rev. E, **66**, 056108 (2002).
26. F. Ben-Adda and J. Cresson. Appl. Math. Comput. **161**, 323 (2005).
27. M.V. Berry and J.P. Keating. SIAM Rev. **41**, 236 (1999).
28. A. Connes. Selecta Math. (N.S.), **5**, 29 (1999).
29. K. Sabbagh. The Riemann hypothesis: The greatest unsolved problem in mathematics. Farrar, Straus and Giroux, New York. 2002.
30. Z. Ahmed and S.R. Jain. Mod. Phys. Lett. A, **21**, 331 (2006).
31. A. Shudo, Y. Shimizu, P. Šeba, H.-J. Stöckmann, and K. Życzkowski. Phys. Rev. E, **49**, 3748 (1994).
32. M.L. Lapidus and M. van Frankenhuysen. Fractal geometry and number theory: Complex dimensions of fractal strings and zeros of zeta functions. Birkhauser, Boston. 2000.